Check for updates

Effects of oxygen on the structural evolution of polyacrylonitrile fibers during rapid thermal treatment†

Liang Chen,[a] Zhigang Shen,[b] Jie Liu,[ac] Jieying Liang[a] and Xiaoxu Wang [ID] *[ac]

In this study, the mechanism of stabilizing polyacrylonitrile (PAN) fibers in a short period of time is investigated through probing the effects of oxygen on the structural evolution of PAN under different temperature regimes. It has been found that oxygen has a significant influence on both the chemical and physical structural evolution of PAN fibers, even in a short period of stabilization time, and the influences are dissimilar at different stabilization temperatures. At lower temperatures (below 140 °C), there is no noticeable change in the chemical and physical structures of the PAN fibers. In the mid-temperature range (140–200 °C), oxygen can slightly induce the cross-linking of PAN chains and result in a higher rate of decreasing crystallinity. When the main chemical reactions are initiated at higher temperatures (200–260 °C), oxygen is directly involved in the oxidation reaction of the PAN chains and facilitates cyclization and dehydrogenation. These reactions initiate in the amorphous regions of PAN fibers, and extend to the crystalline regions at elevated temperatures.

1. Introduction

Polyacrylonitrile (PAN) is the primary precursor to prepare high-performance carbon fibers.[1,2] The manufacture of PAN-based carbon fibers typically involves three main processes: spinning of PAN precursor fibers, thermal oxidative stabilization, and carbonization.[3] The stabilization is the most essential step since the structural integrity of stabilized fibers significantly influences the mechanical properties of the resultant carbon fibers.[4–6] However, the structural evolution of PAN during stabilization is a complex process, and the reaction mechanism is still not clearly understood.[7] As a result, the determination of processing parameters during stabilization is largely empirical, and the stabilization conventionally takes a long time (30–60 min). In recent years, academic and industrial researchers have devoted greater efforts to lower the production cost of carbon fibers through shortening the stabilization time. Thus, having a better understanding of the structural evolution of PAN fibers during rapid stabilization is of great importance for improving the stabilization efficiency.

Oxygen plays an essential role on both physical and chemical structural changes in PAN fibers during stabilization. The stabilization mechanism can be investigated through probing the effects of oxygen on the structural evolution of PAN.[8] It is commonly recognized that the presence of oxygen not only directly affects the oxidation reaction and the cross-linking reaction, but also facilitates the cyclization and dehydrogenation reactions.[9,10] Recently, Liu *et al.* report that the evolutions of chemical and physical structures during thermal oxidative stabilization are simultaneous and interactive, and their transformation mechanism are dissimilar at different temperatures.[11] Yu and co-workers present the rate of oxygen uptake in stabilized PAN fibers have parabolic relationship with time at different temperatures.[12] However, because the oxidation reaction is a diffusion-controlled process, the stabilization time of these studies are generally long in order to gain adequate oxygen uptake.[13,14] It should be noted that based on isothermal DSC studies of PAN fiber under air flow, the main exothermic reactions of PAN fibers are executed in several minutes.[15–18] The rapid exothermic reaction of PAN fibers reveal the potential of substantially shortening the stabilization time. In-depth studies on the stabilization mechanism in short period of stabilization time is essential.

In this study, PAN fibers are rapidly stabilized at different temperatures. The effects of oxygen on the structural evolution of PAN fibers are studied through comparing the chemical and physical structures of PAN fibers stabilized in air and nitrogen atmosphere, which will reflect in mechanical properties of stabilized fibers. The chemical and physical parameters, such as the characteristic functional groups and the crystalline

[a] Key Laboratory of Carbon Fiber and Functional Polymers, Ministry of Education, Beijing University of Chemical Technology, Chao-Yang District, Beijing 100029, China. E-mail: wangxiaoxu@mail.buct.edu.cn

[b] SINOPEC Shanghai Research Institute of Petrochemical Technology, 1658 Pudong North Road, Pudong District, Shanghai, 201208, China

[c] Changzhou Institute of Advanced Materials, Beijing University of Chemical Technology, Changzhou, Jiangsu 213164, China

structures, of PAN fibers stabilized at different temperatures are quantitatively analyzed by density, elemental analysis, FT-IR, NMR, XRD and DSC.

2.   Experimental

2.1   Materials

The PAN precursor fibers (SAF, 6K, 1.22 d/tex) was provided by Courtauld company from UK, and the comonomer components included AN (92.8%), MA (6.0%) and IA (1.2%).

2.2   Thermal treatments

PAN fibers were thermally stabilized in air or nitrogen for 4 min with fixed ends. The stabilization temperature varied from 80 °C to 260 °C with an interval of 20 °C. The PAN fibers stabilized in air or nitrogen atmosphere were denoted as Air-SFs or N_2-SFs, respectively.

2.3   Characterizations

The bulk density of stabilized fibers was measured by a density gradient column filled with tetrachloromethane and hexamethylene at 23 ± 0.1 °C. The testing accuracy was 0.0001 g cm^{-3}. The oxygen contents in stabilized PAN fibers were determined by a vario EL cube elemental analysis instrument (Germany).

The infrared spectra of PAN precursor and stabilized fibers were obtained with the help of a PerkinElmer FT-IR spectrometer II apparatus, based on KBr pellet mode. The results were recorded in 36 scans in combined scan direction from 4000–400 cm^{-1} with resolution of 4 cm^{-1}. The quantitative calculation was carried out by the following formulae:

$$\text{Fraction of reacted nitriles} = \frac{n \times \text{Abs}(1590)}{n \times \text{Abs}(1590) + \text{Abs}(2244)} \times 100\% \quad (1)$$

$$\text{Dehydrogenation index} = \frac{\text{Abs}(1360)}{\text{Abs}(1454)} \times 100\% \quad (2)$$

where n is generally equal to 0.29.[19] Abs (1590) and Abs (2243) refer to the absorbance of conjugated nitrile groups (–C≡N–) and suspended nitrile groups (–C≡N) in the FT-IR spectrum, respectively. Abs (1360) and Abs (1454) are the absorbance of C–H and –CH$_2$– groups,[20] respectively. ^{13}C solid state NMR spectra were measured on Bruker Avance 300 MHz instrument operating at 75.5 MHz by cross-polarization and magic angle spinning (CP/MAS), which equipped with ^{1}H–^{13}C double resonance 4 mm probe. The recycle delay and cross polarization time were set to 6 s and 4 ms, respectively. Magic angle spinning frequency was set to 12 kHz and the spectral width was 30 kHz.

The XRD patterns were obtained by using a D/Max-2500 PC X-ray diffractometer with Cu Kα ($\lambda = 0.1542$ nm) radiation at a voltage of 40 kV, a current of 40 mA and a scanning range from 5–60°. The crystalline size (L_C) was determined by the Scherrer formula:

$$L_C = \frac{k\lambda}{\beta \cos \theta} \quad (3)$$

where λ is the X-ray wavelength with 0.1542 nm, θ is the Bragg angle, β is full width at half maximum (FWHM) of the diffraction peak, and the k value is a constant of 0.89.[21]

Differential scanning calorimetry (METTLER Toledo DSC-822, Mettler-Toledo, Switzerland) was used to perform exothermic reaction behavior analysis. About 5 mg for each sample was measured at temperature ranged from 50 to 440 °C at the heating rate of 5 °C min^{-1} under air flow. Main text of the article should appear here with headings as appropriate.

The tensile strength was measured on XQ-1A Fiber Tensile Tester at a pulling rate of 20 mm min^{-1}. The initial length was set of the sample at 20 mm. For each sample, around 35 tests on single fiber were carried out and results represent averages of 30 tests.

3.   Results and discussion

3.1   Density and oxygen content analysis

During the thermal oxidative stabilization, the evolution of chemical and physical structures of PAN fiber associate with the density changes of the stabilized fibers. Therefore, the density is typically applied to evaluate the degree of stabilization of PAN fibers.[22]

The densities of PAN fibers stabilized in air (Air-SFs) and in nitrogen (N_2-SFs) are plotted in Fig. 1a. For both curves, the plots can be divided into three stages: the low-temperature range from ambient to 140 °C, the mid-temperature range of 140–200 °C, and the high-temperature range of 200–260 °C. In the low-temperature range, the densities of stabilized fibers are comparable with that of PAN precursors, suggesting that there are no significant structural changes below 140 °C. The densities of Air-SFs and N_2-SFs increase from 1.18 g cm^{-3} to 1.19 g cm^{-3} at 160 °C, which is typically originated from the relaxations and/or thermal transitions of PAN molecules in the amorphous and para-crystalline phases of PAN fibers.[23] There is no noticeable difference between the densities of Air-SFs and N_2-SFs below 200 °C, indicating limited influence of oxygen on the fiber density. However, at higher temperatures (above 220 °C), the densities of Air-SFs grow much faster than that of N_2-SFs, which can be attributed to the sharp increase of oxygen uptake as a result of oxidation reaction.[24]
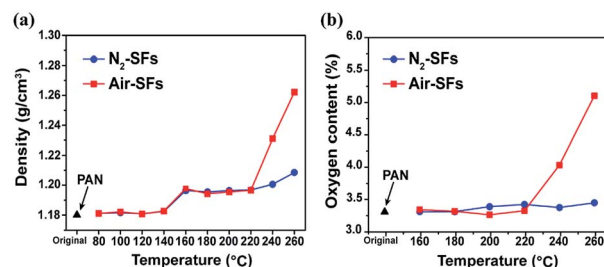

Fig. 1 (a) Densities and (b) oxygen contents of PAN fibers thermally stabilized in air or nitrogen atmosphere.

In order to further justify the above speculation, elemental analysis is applied to directly analyze the oxygen contents in the stabilized fibers. As shown in Fig. 1b, the oxygen contents of Air-SFs and N₂-SFs remain unchanged in the mid-temperature range while that of Air-SFs starts to increase at 220 °C, confirming that PAN fibers have oxygen-uptake reaction over the high temperature range.[24] Additionally, the trends of the oxygen content at higher temperatures are consistent with that of the density change, suggesting that the increase of density is mainly due to the large amount of oxygen uptake during the oxidation process.

3.2 Analysis of chemical and physical structures

Fig. 2a and b show a series of the transmission FT-IR spectra for PAN precursors and stabilized PAN fibers. The absorption bands at 2925 and 1454 cm^{-1} are assigned to $-CH_2-$ units.[20] The single and sharp band at 2243 cm^{-1} is assigned to saturated nitrile groups, and the peak at 1734 cm^{-1} is assigned to carbonyl groups from MA and IA comonomers. In general, the FT-IR spectra of Air-SFs and N₂-SFs are comparable when the stabilization temperature is below 220 °C. As the temperature is increased, a shoulder peak at 1660 cm^{-1} and a strong absorption band at 1600 cm^{-1} emerge for Air-SFs, corresponding to the formation of conjugated carbonyl and aromatic structures due to high degree of cyclization and dehydrogenation.[21] On the other hand, for N₂-SFs, the absorption band at 1590 cm^{-1} enhance gradually along with the increase of temperature, indicating the conversion of nitrile groups in absence of oxygen.[22]

The effect of oxygen on the chemical structure of PAN fibers at different temperatures can be quantitatively inferred using the fraction of reacted nitriles (FNs) (Fig. 2c) and the dehydrogenation index (Fig. 2d), which are calculated based on the ratio of characteristic absorption band in FT-IR spectra. It is observed that the FNs of Air-SFs are slightly higher than that of N₂-SFs at

160–200 °C, indicating oxygen can promote the conversion of nitrile groups in the mid-temperature range. This promotion effect is more pronounced at higher temperatures, in which the main reaction of cyclization is initiated. Similar trends can be found at the plots of dehydrogenation index in Fig. 2d, which reveal that the presence of oxygen can facilitate both the cyclization and the dehydrogenation of PAN in the middle and high temperature ranges.

In order to further explore the effects of oxygen, the ^{13}C ss-NMR is conducted on PAN precursors together with stabilized PAN fibers. The NMR curves of Air-SFs and N₂-SFs stabilized at 260 °C are shown in Fig. 3. Apparently, there are several new resonances appear in the NMR spectrum of Air-SFs (260 °C), suggesting that the chemical structures of PAN fibers stabilized with oxygen are different from that of PAN fibers stabilized in nitrogen. The assignments of these resonances are summarized in Table 1.[23]

The generally accepted assumption is that PAN stabilized with oxygen form the laddered structures with conjugated six-membered aromatic rings and partially cross-linked or oxidized rings.[24,25] On the other hand, PAN stabilized without oxygen experience an aromatization reaction to form oligomeric chains mainly composed of isolated pyridine units connected by alkyl segments.[26,27] It is noteworthy that in the mid-temperature range, despite the FNs of Air-SFs is slightly higher than that of N₂-SFs, their densities are identical. Since oxygen affects not only the chemical structure but also the physical structure of PAN fibers, the physical structural transition may play an important role on compensating the differences of chemical structural changes.

X-ray diffraction pattern may provide information about the crystallinity and the crystalline size of PAN fibers, and the transition of the physical structure of PAN fibers at different temperatures could be inferred based on these parameters. It can be seen from Fig. 4a that the amorphous scattering peak of Air-SFs at $2\theta \approx 25.5°$ became more obvious with the increase of temperature. However, no noticeable change of the amorphous peaks of N₂-SFs (Fig. 4b) is identified, indicating oxygen may disturb the transition of the crystalline structure of PAN fibers.[7,8]

The crystallinity and the crystalline size (L_C) are calculated based on the main diffraction peak at $2\theta \approx 17°$, as shown in
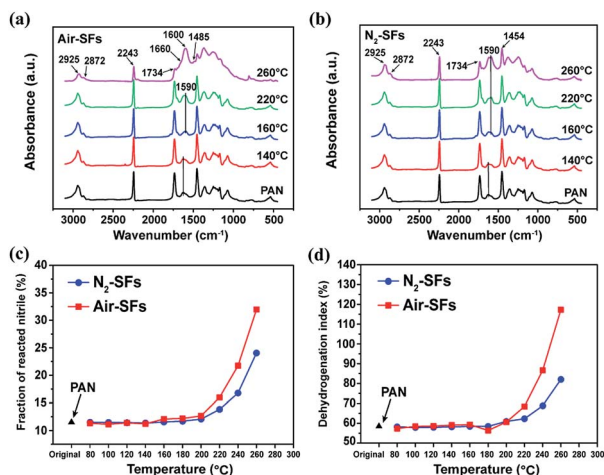

Fig. 2 FT-IR spectra of (a) Air-SFs (260 °C, 220 °C, 160 °C and 140 °C), and (b) N₂-SFs (260 °C, 220 °C, 160 °C and 140 °C) (c) fraction of reacted nitrile groups (FNs) as a function of stabilization temperature (d) dehydrogenation index as a function of stabilization temperature.
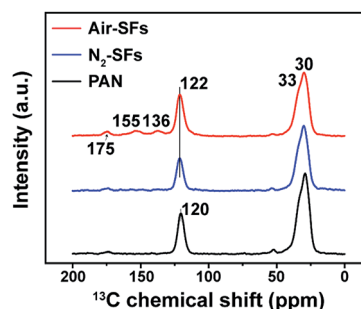

Fig. 3 ^{13}C ss-NMR spectra of PAN precursor, Air-SFs (260 °C) and N₂-SFs (260 °C).

Table 1 Typical ^{13}C NMR resonances in solid PAN precursor and stabilized PAN fibers

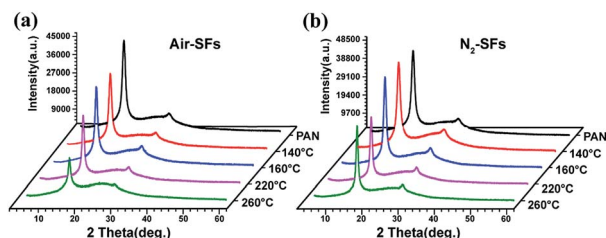| Functional groups	^{13}C chemical shift (ppm)
Methine –CH<	30
Methylene –CH$_2$–	33
C≡N (saturated)	120
C≡N (unsaturated)	122
>C=C< (backbone)	115, 136
C=N, C=C mix	155
Carbonyl C=O	175

Fig. 4 (a) X-ray diffraction patterns of PAN fibers and Air–SFs (b) X-ray diffraction patterns of PAN fibers and N$_2$-SFs.

Fig. 5a and b, respectively. The crystallinity of Air-SFs decreases rapidly from 160 °C to 200 °C. On the other hand, N$_2$-SFs samples demonstrate a delayed decrease of crystallinity in the mid-temperature range and the change of crystallinity is smaller than that of Air-SFs. The higher crystallinity reduction of Air-SFs can be explained by the oxygen-induced intermolecular crosslinking, which decompose the ordered region of PAN para-crystalline.[28]

Despite a decrease of crystallinity in the mid-temperature range, the crystalline size for both Air-SFs and N$_2$-SFs increase in the middle and the high temperature ranges (Fig. 5b). Similar observations have been reported in previous studies, which attribute the growth of PAN crystallite to the transitions of disordered structure to the para-crystalline structure.[29] Additionally, birefringence measurements on solvent-cast PAN films reveal that recrystallization would take place in PAN around 140 °C.[30,31] Considering the fact that Air-SFs has slightly higher FNs and lower crystallinity than N$_2$-SFs at 140–200 °C, we can arguably assume that the small amount of oxygen-induced
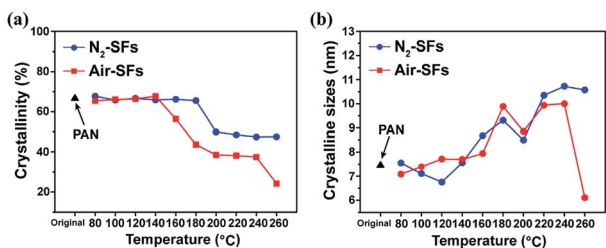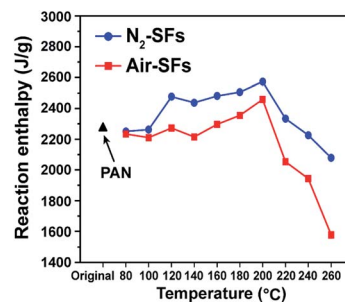
crosslinking between PAN chains hinder the recrystallization of PAN during their cooling process after stabilization, as indicated by the lower crystallinity of Air-SFs. On the other hand, for un-crosslinked PAN chains, their recrystallization behaviors are not affected by oxygen and therefore similar crystalline sizes have been observed between Air-SFs and N$_2$-SFs in the mid-temperature range (Fig. 5b).

Generally, the chemical reactions of PAN would interfere the structural regulation of PAN chains. However, it is interesting to note that although the main nitrile reactions have already been initiated for both Air-SFs and N$_2$-SFs at 200–240 °C, their crystallinities are retained and their crystalline size are even increasing. These suggest that the crystalline region within PAN fibers is not affected by the ongoing chemical reactions. Since the stabilization process take only 4 min in this study, the chemical reactions initiated in the amorphous region of PAN fibers do not affect the ordered regions below 240 °C. However, when the stabilization temperature is above 240 °C, both the crystallinity and the crystalline size of PAN fibers decrease, indicating the reactions have extended to the crystalline region of PAN fibers at higher temperatures.

3.3 Analysis of exothermal properties

The chemical reactions involved in the stabilization of PAN fibers are generally exothermic.[32] The above effects of oxygen on the evolution of the chemical and physical structures of PAN fibers during the rapid thermal stabilization can be further investigated by their exothermic reaction behavior. The DSC curves of stabilized fibers are shown in Fig. S1 of ESI.† The reaction enthalpy (Q_p) of the stabilized fibers are calculated based on the DSC curves and are plotted in Fig. 6. It can be seen that the Q_p of stabilized fibers increase in the low- and mid-temperature range. However, there is a sudden drop of Q_p for both Air-SFs and N$_2$-SFs when the stabilization temperature is above 200 °C.

The Q_p is associated with the main exothermal reactions of PAN fibers. Thus, the exothermal behavior of Air-SFs and N$_2$-SFs can also be explained by our previous assumptions that: (1) the intermediate structures (oxygen-induced crosslinking) may have formed below 200 °C, which convert adjacent nitriles and release a small portion of reaction heat; (2) the increased crystalline size in the mid-temperature range may result in the

Fig. 5 (a) Crystallinity of Air-SFs and N$_2$-SFs, (b) crystalline sizes (L_C) of Air-SFs and N$_2$-SFs as a function of stabilization temperature.

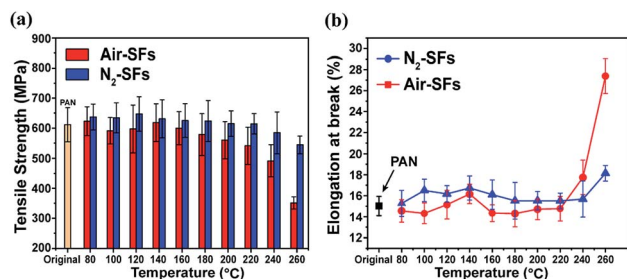**Fig. 6** Reactions enthalpies of Air-SFs and N$_2$-SFs as a function of stabilization temperature.

Fig. 7 (a) Tensile strength of Air-SFs and N$_2$-SFs as a function of stabilization temperature, (b) elongation at break of Air-SFs and N$_2$-SFs as a function of stabilization temperature.

increased Q_p for both Air-SFs and N$_2$-SFs, and the lower crystallinity of Air-SFs may account for its lower Q_p compared with that of N$_2$-SFs; (3) the main exothermal reaction of PAN in the high-temperature range could release considerable amount of reaction heat, which result in the sudden drop of Q_p for both the Air-SFs and N$_2$-SFs samples.

3.4 Analysis of mechanical properties of stabilized fibers

Fig. 7a and b illustrate the different trends of mechanical properties of Air-SFs and N$_2$-SFs. In the low and mid temperature range, the effects of oxygen on the stabilized fibers are not obvious while the tensile strength of Air-SFs drops dramatically in the high temperature range (Fig. 7a).

It is well known that when unsaturated nitrile units (–C≡N) are convert into saturated nitrile group (–C=N–) with the progress of FNs, cohesive energy between the polyacrylonitrile chains drops significantly.[33,34] The above discussions suggest that the presence of oxygen will appreciably accelerate the structural transformations in the high temperature, which means that Air-SFs will gain higher FNs, dehydrogenation index and lower crystallinity. This will cause the more loss of cohesive energy. Therefore, the tensile strength of Air-SFs is less strong than that of N$_2$-SFs.

4. Conclusions

In summary, oxygen has significant influences on both the chemical and physical structural evolutions of PAN fibers even during a short period of thermal stabilization, and the influence is diverse at different stabilization temperatures. At lower temperatures (below 140 °C), there is no noticeable change of chemical and physical structures of PAN fibers based on FT-IR and XRD results. As the temperature is increased from 140 to 200 °C, oxygen can slightly induce the initial reaction of nitrile groups and the crosslinking of PAN chains, which result in higher decreasing rate of crystallinity. At higher temperatures (200–260 °C), the main cyclization reaction and dehydrogenation reactions are facilitated by the presence of oxygen, and oxygen directly participate in the oxidation reaction of PAN chains. These reactions initiate in the amorphous regions of PAN fibers, and extend to the ordered regions at elevated temperatures. Oxygen consequently results in the remarkable

diminishing of tensile strength of stabilized fibers at higher temperatures.

Conflicts of interest

There are no conflicts to declare.

Acknowledgements

References

1 E. Frank, L. M. Steudle, D. Ingildeev, J. M. Spörl and M. R. Buchmeiser, *Angew. Chem., Int. Ed.*, 2014, **53**, 5262.

2 P. Wang, J. Liu and R. Li, *J. Appl. Polym. Sci.*, 1994, **52**, 1667.

3 X. Huang, *Materials*, 2009, **2**, 2369.

4 P. Wang, J. Liu, Z. Yue and R. Li, *Carbon*, 1992, **30**, 113.

5 W. X. Zhang, J. Liu and G. Wu, *Carbon*, 2003, **41**, 2805.

6 S. C. Martina, J. J. Liggata and C. E. Snapeb, *Polym. Bull.*, 2010, **64**, 497.

7 Z. Fu, B. Liu, L. Sun and H. Zhang, *Polym. Degrad. Stab.*, 2017, **140**, 104.

8 H. Chen, Y. Pan, S. Hou, Z. Shao, Y. Hong and A. Ju, *RSC Adv.*, 2017, **7**, 54142.

9 S. Xiao, B. Wang, C. Zhao, L. Xu and B. Chen, *J. Appl. Polym. Sci.*, 2012, **127**, 2332.

10 Y. Xue, J. Liu, F. Lian and J. Y. Liang, *Polym. Degrad. Stab.*, 2013, **98**, 2259.

11 C. Liu, L. Hu, Y. Lu and W. Zhao, *J. Appl. Polym. Sci.*, 2015, **132**, 42182.

12 M. J. Yu, C. G. Wang, Y. J. Bai, Y. Xu and Z. Bo, *J. Appl. Polym. Sci.*, 2008, **107**, 1939.

13 J. Wang, L. Y. Hu, C. L. Yang, W. Z. Zhao and Y. G. Lu, *RSC Adv.*, 2016, **6**, 73404.

14 L. A. Beltz and R. R. Gustafson, *Carbon*, 1996, **34**, 561.

15 H. Kakida and K. Tashiro, *Polym. J.*, 1997, **29**, 557.

16 R. Schierholz, D. Kröger, H. Weinrich, M. Gehring, H. Tempel, H. Kungl, J. Mayer and R.-A. Eichel, *RSC Adv.*, 2019, **9**, 6267.

17 H. Kakida and K. Tashiro, *Polym. J.*, 1996, **28**, 30.

18 R. Devasia, C. P. Reghunadhan Nair, P. Sivadasan, B. Katherine and K. N. Ninan, *J. Appl. Polym. Sci.*, 2003, **88**, 915.

19 G. L. Collins, N. W. Thoma and G. E. Williams, *Carbon*, 1988, **26**, 671.

20 S. Nunna, M. Naebe, N. Hameed, C. Creighton, S. Naghashian, M. J. Jennings, S. Atkiss, M. Setty and B. L. Fox, *Polym. Degrad. Stab.*, 2016, **125**, 105.

21 J. B. Nichols, *J. Appl. Phys.*, 1954, **25**, 840.

22 T. Q. Sun, Y. P. Hou and H. J. Wang, *J. Appl. Polym. Sci.*, 2010, **118**, 462.

23 D. Sawai, T. Kanamoto, H. Yamazaki and K. Hisatani, *Macromolecules*, 2004, **37**, 2839.

24 T. Usami, T. Itoh, H. Ohtani and S. Tsuge, *Macromolecules*, 1990, **23**, 2460.

25 Y. Wang, L. Xu, M. Wang, W. Pang and X. Ge, *Macromolecules*, 2014, **47**, 3901.

26 X. Liu, W. Chen, Y. L. Hong, S. Yuan, S. Kuroki and T. Miyoshi, *Macromolecules*, 2015, **48**, 5300.

27 X. Liu, Y. Makita, Y. Hong, Y. Nishiyama and T. Miyoshi, *Macromolecules*, 2017, **50**, 244.

28 Z. Yang, H. Peng, W. Wang and T. Liu, *J. Appl. Polym. Sci.*, 2010, **116**, 2658.

29 F. Lian, J. Liu, Z. Ma and J. Y. Liang, *Carbon*, 2012, **50**, 488.

30 R. M. Kimmel and R. D. Andrews, *J. Appl. Phys.*, 1965, **36**, 3063.

31 Z. Bashir, *J. Macromol. Sci., Part B: Phys.*, 2007, **40**, 37.

32 Z. Fu, B. Liu, L. Sun, Y. Deng and H. Zhang, *Polym. Adv. Technol.*, 2017, **28**, 1662.

33 O. P. Bahl and L. M. Manocha, *Carbon*, 1974, **12**, 417.

34 I. Karacan and G. Erdoğan, *Fibers Polym.*, 2012, **13**, 855.